Atmospheric electric field variations and lower ionosphere disturbance during the Total Solar Eclipse of 2010 July 11

José C. Tacza[a,*], Jean-Pierre Raulin[a], Edith L. Macotela[a], Edmundo O. Norabuena[b], Germán Fernandez[c]

[a] Centro de Rádio Astronomia e Astrofísica Mackenzie (CRAAM), Escola de Engenharia, Universidade Presbiteriana Mackenzie, São Paulo, 01302-907 SP, Brasil.
[b] Instituto Geofísico del Perú, IGP, Lima, Peru
[c] Complejo Astronómico El Leoncito, CASLEO, San Juan, Argentina.
[*] Corresponding Author. Fax: +55 11 32142300.
E-mail address: josect1986@gmail.com

Key Points:

- Changes of atmospheric electric field during a total solar eclipse.
- Electric field and VLF phase time histories are similar.
- Possible connection between the lower ionosphere and the lower atmosphere.

Abstract

In this paper, we study the variations of atmospheric electric field during the total solar eclipse (TSE) of July 11, 2010, at Complejo Astronómico El Leoncito (CASLEO). These variations observed with two identical sensors separated by 0.4 km, show a significant increase (~55 V/m) when compared with averaged values measured during previous and subsequent fair weather days. Furthermore, identical changes are detected on the measured phases of Very Low Frequency waves received at CASLEO. The latter suggests a possible connection between the lower ionosphere and the lower atmosphere during the period of the eclipse.

Keywords Atmospheric Electric Field, Fair-Weather, Total Solar Eclipse, Very Low Frequency waves.

1. - Introduction

The atmospheric electric field persists in fair weather[1] regions mainly due to thunderstorms occurring at remote locations. This is part of the current knowledge of the global atmospheric electric circuit (GAEC). In short, the GAEC relates the charge separation in regions of disturbed weather to electrical current flowing in fair weather regions. Recent advances on study of the GAEC are reviewed in Williams and Mareev (2014).

The atmospheric electric field in fair weather regions is affected by several phenomena, such as for example, solar and seismic activities (see references in Tacza et al., 2014). Investigations of the effects of solar eclipses on the atmospheric electric field have also been reported for a long time. Previous studies showed an increase of the atmospheric electric field (Anderson and Dolezalek, 1972; Dhanorkar et al., 1989; De et al., 2009), while other reports mention a decrease (Jones and Gieseck, 1944; Markson and Kamra, 1971; Kamra and Varshneya, 1967; Retalis, 1981; Kamra et al., 1982; Manohar et al., 1995; Babakhanov et al., 2013; De et al., 2013; Kumar et al., 2013). Finally, few studies do report no change at all (Freier, 1960). Inconsistency of the effects of a solar

[1] Fair weather conditions are those in which no local electrification processes are occurring, without appreciable convective cloud extent (Harrison, 2013).

eclipse on atmospheric electricity may occur because of different instrumentations and local meteorological conditions during observations (Babakhanov et al., 2013).

Two factors have been proposed to explain the effect of the eclipse on atmospheric electrical parameters. These are, changes in upper atmosphere processes (e.g. Koenigsfeld, 1953; Dhanorkar et al., 1989; De et al., 2009; Kumar et al., 2013; Babakhanov et al., 2013) or changes in atmospheric boundary layer processes close to ground surface (e.g. Jones and Gieseck, 1944; Gish, 1944; Anderson, 1972; Anderson and Dolezalek, 1972; Kamra et al., 1982).

With respect to processes in the upper atmosphere, Koenigsfeld (1953) suggests that variations in the amount and height of ozone influence the amount of ultraviolet radiation absorbed and reduce the electrical conductivity of the atmosphere. In addition, the author mentions that the ionization of ice crystals by ultraviolet photons should result in change of the electrical conductivity. De et al. (2009) suggest that the removal of electrons from the lower ionosphere due to recombination during the solar eclipse may give rise to an increase in the electrical field.

With respect to changes in atmospheric boundary layer, Anderson and Dolezalek (1972) propose a mechanism to determine the variation of the electric field intensity. The attenuation of solar radiation due to an eclipse causes a reduction in the turbulent activity (or eddies) starting at the lowest levels of the atmosphere and propagating upward. After a series of processes, a downward convection current of heavy positive ions is established. The latter, causes a reduction in electrical conductivity and therefore produces an increase in the atmospheric electric field. Jones and Giesecke (1944) also proposed a similar mechanism.

In this paper, we study the variations of atmospheric electric field during the total solar eclipse (TSE) on July 11, 2010 at Complejo Astronómico El Leoncito (CASLEO), Argentina (Lat. 31.798°S, Long. 69.295°W, Altitude: 2550 masl). Section 2 presents the instrumentation and data treatment. In Section 3 we present our results by comparing the effects of the TSE on both electric field records, and VLF phase measurements. Section 4 is devoted to the discussion of our findings, and in Section 5 we give our concluding remarks.

2. - Instrumentation

Continuous measurements of atmospheric electric field are being recorded with two sensors located in CASLEO (CAS1 and CAS2), ~0.4 km apart. Each sensor consists of a commercially manufactured (Boltek Corporation EFM100-1000120-050205) electric field mill (EFM) and is part of a network of electric field sensors installed in South America. Some important technical specifications of the sensor EFM are the electric field dynamic range between $\pm$ 20 kV/m and a response time of 0.1 s. The principle of EFM operation is based on the fundamental laws of electromagnetism. When a conducting plate is exposed to an electric field, a charge is induced proportional to the electric field and the area of the plate (Tacza, 2015). Electric field measurements are recorded with a time resolution of 0.5 s, and afterwards integrated using 30 min averages for the analysis reported here. The electric field intensities are previously corrected to account for the height of the local instrument (sensor) mounting. This is because the latter results in overestimated readings (Tacza et al., 2014).

The database of VLF signals is provided by the South American VLF Network (SAVNET) (Raulin et al. 2009). In this work we use the VLF propagation path between transmitter (NPM; Hawaii; f=21.4 kHz) and the receiver CAS (CASLEO). The transmitted wave propagates within the Earth-Ionosphere waveguide to the receiver CAS. Phase and amplitude of the VLF wave are recorded with 1 s time resolution. This allows one to monitor the height of the quiescent D-region of the ionosphere at ~ 70 km.

3. - Observations

The path of the TSE on July 11, 2010 over the Earth's surface is illustrated in figure 1. The trajectory of the umbra and penumbra are represented by a sequence of filled circles and by solid lines, respectively. The TSE has is first contact on the Earth's surface at 17:10 UT and ended at 21:58 UT. The percentage of maximum obscurity over CASLEO was of 41.73 %. The end of the eclipse coincides with the sunset in CASLEO (21:50 UT). The local circumstances of the eclipse were obtained from http://xjubier.free.fr/en/site_pages/SolarEclipseCalculator.html.

Figure 2 shows the daily variations of the atmospheric electric field obtained by the two sensors, for the day of the eclipse (July 11), a day before (July 10), a day after (July 13) and the mean curve obtained from nine days of fair weather[2] observations in July. July 12 was not selected because of local weather disturbances. Averages are calculated every 30 minutes as well as the corresponding standard deviation σ_q and the error bars in Figure 2 represent $2\sigma_q$. The dashed blue lines represent the first contact time and ending time of the eclipse. CAS1 and CAS2 electric field measurements show a clear deviation from the mean curve during the period starting around 18:30 UT and ending at 22 UT.

This deviation is even more evident in Figure 3, where we show the difference between the electric field curve recorded on the day of the eclipse, and the averaged fair weather curve. In this Figure we use error bars of 1σ. We first calculate the standard deviation σ_e of the average electric field value over 30 minutes for the day of the eclipse. Then the standard deviation σ is given by $\sigma_q + \sigma_e$. The effect of the eclipse on the electric field values is approximately 55 V/m for both sensors. This is equivalent to an excess of about 44 % over the mean value (130 V/m). The atmospheric electric field starts to increase from about 18:30 UT and reaches its maximum at 20:30 UT, before progressively decreases until to reach values of fair weather's days. Therefore, the observed effect on the electric field values is well above the standard deviation.

Similarly, Figure 4 shows the cumulative frequency of the CAS2 electric field values averaged each 30 minutes during the period 10-24 UT. The red, black and blue lines represent the values for the day of the eclipse, the monthly (9 days) and the seasonal (42 days) mean curves of fair weather days, respectively. We note that for the average curves, 100 % of electric field values are lower than 130 V/m. On the other hand, for the day of the eclipse on July 11 25% of the records are greater than 130 V/m.

The effect of the eclipse has also been detected in the analysis of Very Low Frequency (VLF) signals (Macotela, 2015 and references therein). Macotela (2015) estimated the phase variation in VLF signals during the TSE July 11, 2010 using the propagation path NPM-CAS from the transmitter NPM (Hawaii) to the receiver CAS. The upper panel of Figure 5 shows the diurnal phase variation observed on the eclipse day (red curve) compared with a quiet mean curve (black curve) obtained from undisturbed days. The eclipse effect is shown in the bottom panel using a simple difference.

Therefore, in figure 5, we note a clear eclipse effect on the VLF signal. Significant deviation of the normal diurnal phase variation started around 18:20 UT and lasted approximately 3h10m. The maximum phase deviation was ~20° and it occurred at 20:41 UT. The eclipse effect shows a slow

[2] The criteria for choosing days of fair weather was to select days with atmospheric electric field values in the range of 40-200 V/m, and also, the values have to present a daily variation approximately similar to Carnegie curve (see for example figure 6a in (Harrison, 2013)), that is, with higher electric field values between 12-24 UT compared with values between 00-12 UT.

phase decrease until the maximum, and then a fast recovery to the quiescent level.

Figures 3 and 5 show a strong similarity between the time variability of both the atmospheric electric field and VLF phase measurement.

4. - Discussion

The similarity shown in Figures 3 and 5, and mentioned in the previous section, may indicate the independent responses to a single phenomenon, i.e. the TSE of 2010, July 11. Indeed, the TSE gradually blocks the solar Lyman-α photon flux, and free electrons in the lower ionospheric D-region progressively recombine. This leads to a rise-up of the reflection height, which is observed as a phase (delay) change (Raulin et al., 2010).

On the other hand, as we mentioned in the introduction, the TSE induces changes in local meteorological parameters, as the temperature, which can result in atmospheric electric field variations (Anderson and Dolezalek, 1972; Jones and Giesecke, 1944). Unfortunately, for this particular event, we do not have such meteorological database as to discuss such interpretation.

Cole and Pierce (1965) estimated that 90% of the earth-ionosphere columnar resistance is concentrated below the altitude of 2.4 km. Thus, in principle, ionospheric electrical conductivity changes has no effect on the electric field values recorded on the Earth's surface. However, CASLEO is located at an altitude of 2550 masl. For this reason, and because of the close similarity shown in Figures 3 and 5, we cannot exclude a direct relationship between electric conductivity changes in the ionospheric D-region, and variations of the atmospheric electric field recorded at CASLEO.

In this case, a possible explication to support the above relationship is that the decrease of the electrical conductivity in the ionospheric layer leads to an increase of its positive electric potential. The latter results in an increase of the atmospheric electric field as early proposed by De et al., (2009).

5. - Conclusions

The present study examines the evolution of the atmospheric electric field under the influence of the TSE of July 11, 2010. The results show an increase of electric field during the eclipse period, closely related to similar time variations of the phase of VLF signals. This may indicate two independent manifestations of the effects of the TSE. However, we cannot exclude a causal relationship between electrical conductivity changes in the lower ionosphere, and electric field variations at 2550 masl.

Acknowledgments

Observational electric field and VLF data from this study are available upon request. The work of JT was supported by CAPESP funding agency. JPR thanks CNPq funding agency (Proc. 482000/2011-2 and 312788/2013-4). Authors are grateful to anonymous reviewers for their constructive comments and suggestions, which helped to improve the quality of the paper.

References

Anderson, R.V. (1972), Atmospheric electricity, turbulence and a pseudo-sunrise effect resulting from a solar eclipse, Journal of Atmospheric and Terrestrial Physics, 34, 567-572.
Anderson, R.V., and H. Dolezalek (1972), Atmospheric electricity measurements at Waldorf,

Maryland during the 7 March 1970 solar eclipse, Journal of Atmospheric and Terrestrial Physics, 34, 561-566.
Babakhanov, I.Y., A.Y. Belinskaya, and M.A Bizin (2013), The geophysical disturbances during the total solar eclipse of 1 August 2008 in Novosibirsk, Russia, Journal of Atmospheric and Solar-Terrestrial Physics, 92, 1-6.
Cole, R.K. and Pierce, E.T (1965), Electrification in the Earth's atmosphere for altitude between 0 and 100 kilometers. Journal of Geophysical Research, 70, 2, 2735-2749.
De, S. S., B.K. De, B. Bandyopadhyay, B.K. Sarkar, S. Paul, D.K. Haldar, S. Barui, A. Datta, S.S. Paul, and N. Paul (2009), The effects of solar eclipse of August 1, 2008 on Earth's atmospheric parameters, Pure and Applied Geophysical (Switzerland), 167, 1273, doi: 10.1007/s00024-009-0041-0.
De, S.S., B. Bandyopadhyay, S. Paul, D.K. Haldar, M. Bose, D. Kala, and G. Guha (2013), Atmospheric electric potential gradient at Kolkata durign solar eclipse of 22 July 2009, Indian Journal of Radio & Space Physics, 42, 251-258.
Dhanorkar, S., C.G. Deshpande, and A.K. Kamra, (1989), Atmospheric electricity measurements at Pune during the solar eclipse of 18 March 1988, Journal of Atmospheric and Terrestrial Physics, 51, N° 11/12, 1031-1034.
Freier, G.D. (1960), The Earth's electric field during and eclipse of the sun, Journal of Geophysical Research, 65, 3179-3181.
Gish, O. H. (1944), Discussion of "Atmospheric-Electric Observatories at Huancayo, Peru, during the Solar Eclipse, January 25, 1944", Terr. Magn. Atmos. Electr., 49(2), 123–124, doi: 10.1029/TE049i002p00123.
Harrison, R.G. (2013), The Carnegie curve, Surveys in Geophysics, 34, 2, 209-232, doi: 10.1007/s10712-012-9210-2.
Jones, M.W., and A.A. Giesecke (1944), Atmospheric-Electric Observatories at Huancayo, Peru, during the Solar Eclipse, January 25, 1944, Terr. Magn. Atmos. Electr., 49(2), 119–122, doi: 10.1029/TE049i002p00119.
Kamra, A.K., and N.C. Varshneya (1967), The effect of a solar eclipse on atmospheric potential gradients, Journal of Atmospheric and Terrestrial Physics, 29, 327-329.
Kamra, A.K., J.K. Teotia, and A.B. Sathe (1982), Measurements of electric field and vertical distribution of space charge close to the ground during the solar eclipse of February 16, 1980, Journal of Geophysical Research, 87, 2057-2060.
Koenigsfeld, L. (1953), Investigations of the potential gradient at the earth's ground surface and within the free atmosphere, Thunderstorm electricity, 149, 24-45.
Kumar, C.P.A., R. Gopalsingh, C. Selvaraj, K.U. Nair, H.J. Jayakumar, R. Vishnu, S. Muralidas, and N. Balan (2013), Atmospheric electric parameters and micrometeorological processes during the solar eclipse on 15 January 2010, Journal of Geophysical Research: Atmospheres, 118, 5098-5104, doi: 10.1002/jgrd.50437.
Macotela, E.L. (2015), Contribuição ao estudo de distúrbios ionosféricos utilizando a técnica de VLF, M.S. thesis, Dep. of Geospatial Sciences and Applications, Mackenzie Presbyterian University, São Paulo, Brasil.
Manohar, G. K., S.S. Kandalgaonkar, and M.K. Kulkarni (1995), Impact of a total solar eclipse on surface atmospheric electricity, Journal of Geophysical Research, 100, 20,805-20,814.
Markson, R., and A.K. Kamra (1971) Airborne and ground measurements of the atmospheric potential gradiente during a solar eclipse, Journal of Atmospheric and Terrestrial Physics, 33, 1107-1113.
Raulin, J.-P., P.C.M. Hadano, A.C.V. Saraiva, E. Correia, and P. Kaufmann (2009), The South America VLF NETwork (SAVNET), Earth Moon Planets, 104, 247-261, doi: 10.1007/s11038-008-9269-4.
Raulin, J.-P, Bertoni, F., Gavilan, H., et al. (2010), Solar flare detection sensitivity using the South America VLF NETwork (SAVNET), Journal of Geophysical Research, 115, A07301, doi: 10.1029/2009JA015154.

Retalis, D. (1981) Atmospheric electrical potential gradient measurements during the annular solar eclipse of 29 April 1976, Journal of Atmospheric and Terrestrial Physics, 43, 999-1002.
Tacza, J.C. (2015), Análise do campo elétrico atmosférico durante tempo bom e distúrbios geofísicos, M.S. thesis, Dep. of Geospatial Sciences and Applications, Mackenzie Presbyterian University, São Paulo, Brasil.
Tacza, J.C., J.-P Raulin, E.L. Macotela, E. Norabuena, G. Fernandez, E. Correia, M.J. Rycroft, and R.G. Harrison (2014), A new South American network to study the atmospheric electric field and its variations related to geophysical phenomena, Journal of Atmospheric and Solar-Terrestrial Physics, 120, 70-79.
Williams, E., and E. Mareev (2014) Recent progress on the global electric circuit, Atmospheric Research, 135-136, 208-227.

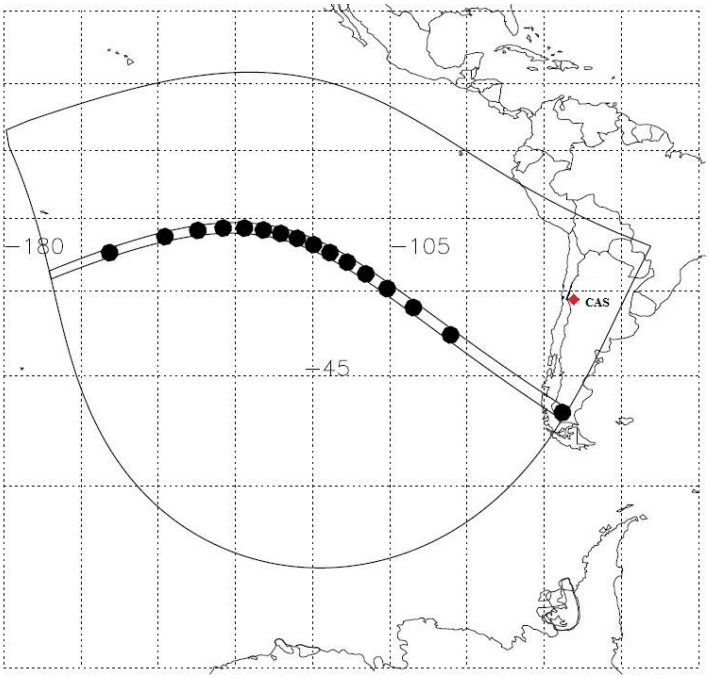

Figure 1. The propagation path of the eclipse on July 11, 2010 on the Earth's surface, showing the trajectory of the umbra (sequence-filled circles) and penumbra (solid lines). Additionally, CAS indicates the location of the sensors (CAS, red diamond).

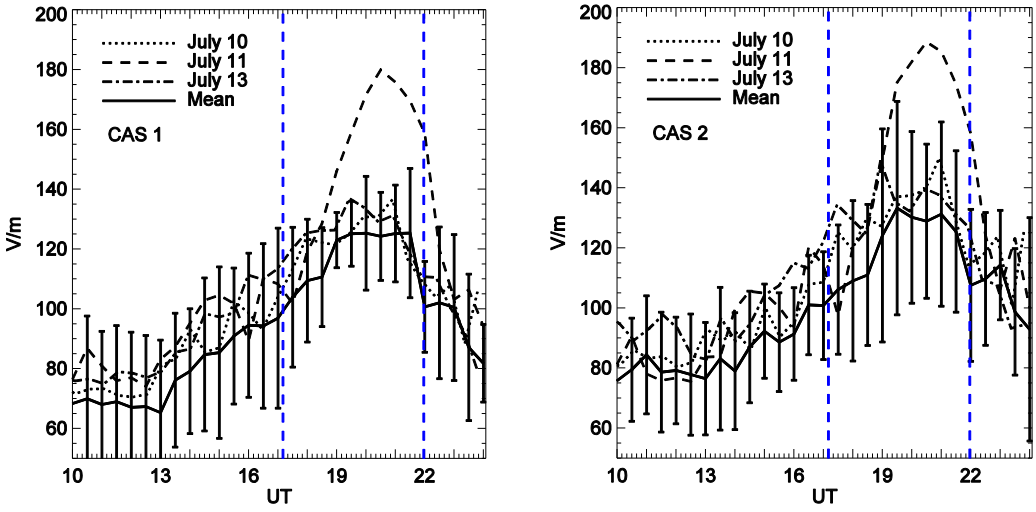

Figure 2. Daily temporal variation of electric field values for the TSE of 11 July 2010 in CAS1 and CAS2 sensors (dashed line), a day before (dotted line), a day after (dash-dotted line) and the monthly mean curve (solid line). The error bars represent the standard deviation (2σ) for the mean curve and dashed blue lines represent the first contact time and ending time of the eclipse.

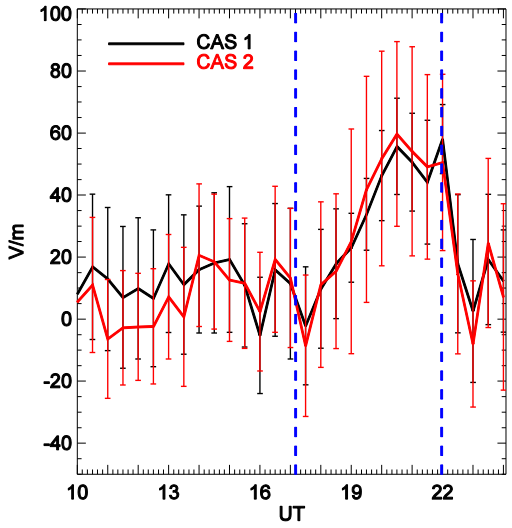

Figure 3. Eclipse effect on the values of the atmospheric electric field, for CAS1 (black line) and CAS2 (red line). The error bars represent the standard deviation 1σ and dashed blue lines represent the first contact time and ending time of the eclipse.

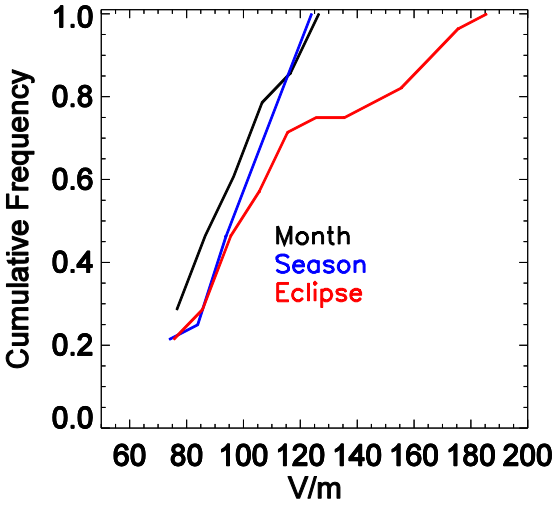

Figure 4. Cumulative frequency to the values of the atmospheric electric field (CAS2 sensor) to the day of the eclipse (red), monthly mean curve (black) and seasonal mean curve (blue color), during the period of 10-24 UT.

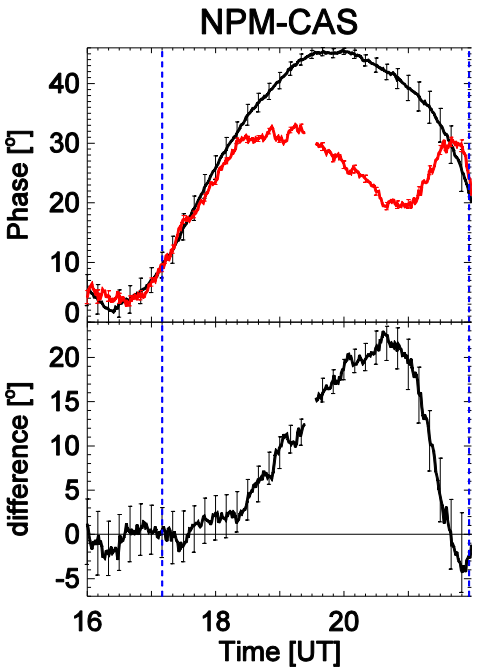

Figure 5. Upper panel: VLF phase variation, for the propagation path NPM-CAS, observed at CASLEO during the eclipse (red curve), compared with that recorded during a typical quiet day (black curve). Bottom panel: The effect of the eclipse estimated from the difference of the two upper curves. The dashed blue lines represent the first contact time and ending time of the eclipse.